



Hydrology, environment

Mineralogical and geochemical study of clay and calcite veins in a shear zone related to a sulphur spring (NW Portugal)

Étude minéralogique et géochimique de veines d'argile et de calcite dans une zone de cisaillement concernant une source sulfureuse

Manuela Fonte Lima, Jorge Pamplona, Maria Amália Sequeira Braga*

Centro de Investigação Geológica, Ordenamento e Valorização de Recursos (CIG-R), Departamento de Ciências da Terra, Universidade do Minho, Campus de Gualtar, 4710-057 Braga, Portugal

ARTICLE INFO

Article history:

Received 25 February 2011

Accepted after revision 24 May 2011

Presented by Ghislain de Marsily

Keywords:

Fracture infillings

Granite weathering

Calcite

Smectite

Isotopic signatures

Sulphur spring

Water–rock interaction

Portugal

Mots clés :

Remplissage de fractures

Altération du granite

Calcite

Smectite

Signatures isotopiques

Source sulfureuse

Interaction eau–roche

Portugal

ABSTRACT

In the Terras de Bouro area, in Northwest Portugal, the role of water–rock interaction, either by the mineralization of the sulphur spring, or by the nature of the granite secondary minerals, was studied as a complement to exploration for mineral water. This approach is justified by the peculiar mineral paragenesis found, which is very different from those of the regional weathering products. Calcite and montmorillonite as veins infilling and pyrite in the wall rock are the secondary minerals characteristic of mineral water occurrence. Sulphur water composition, alkaline pH and low redox potential are some factors that may favour the formation of montmorillonite, calcite and essentially pyrite, in the spring zone. Isotopic signatures in $\delta^2\text{H}$ and $\delta^{18}\text{O}$ of sulphur water show that its origin is dominantly meteoric. Isotopic signatures $\delta^{13}\text{C}$ and $\delta^{18}\text{O}$ of calcite and of the inorganic carbon in the water suggest that calcite precipitates from carbonate species in the sulphur water at $\sim 17^\circ\text{C}$.

© 2011 Académie des sciences. Published by Elsevier Masson SAS. All rights reserved.

R É S U M É

Dans la région de Terras de Bouro (Nord-Ouest Portugal), le rôle de l'interaction eau–roche, soit par la minéralisation de la source sulfureuse, soit par la nature des minéraux secondaires, a été étudié à la suite des travaux d'exploitation des eaux minérales. Cette démarche est justifiée par une paragenèse minérale particulière, laquelle est très différente de celle des produits d'altération météorique régionaux. La calcite et la montmorillonite en tant que remplissage des veines et la pyrite dans l'encaissant sont les minéraux secondaires caractéristiques du site d'occurrence de l'eau minérale. La composition de l'eau sulfureuse, son pH élevé et un bas potentiel redox sont des facteurs qui expliquent la formation, dans la zone d'émergence, de montmorillonite, calcite et particulièrement de pyrite. La signature isotopique $\delta^2\text{H}$ et $\delta^{18}\text{O}$ de l'eau sulfureuse montre une origine météorique dominante. Les analyses isotopiques ($\delta^{13}\text{C}$ et $\delta^{18}\text{O}$) des espèces carbonatées de l'eau et des calcites suggèrent que la calcite a précipité à partir de cette eau dans les conditions de l'émergence ($\sim 17^\circ\text{C}$).

© 2011 Académie des sciences. Publié par Elsevier Masson SAS. Tous droits réservés.

* Corresponding author.

E-mail address: masbraga@dct.uminho.pt (M.A.S. Braga).

1. Introduction

The NW region of Portugal has abundant Variscan granites with an intense fracture network, and strongly weathered. Thermal springs are related to some of these fractures. Concerning mineral water resources, sulphur springs are the most abundant hydrochemical types of continental Portugal and, also, of the Central Iberian Zone (CIZ). Sulphur springs are characterized by alkaline pH, sulphur reduced species and high anomalous contents of silica, fluoride, bromide, boron, ammonium and sodium (Calado, 1993, 2002; Marques, 1999). Near the surface, the instability of the granitic rocks is favourable to the weathering of its primary minerals. Fracture systems in those rocks are one of the factors that control the weathering processes. Chemical elements not incorporated in the secondary framework minerals (e.g., clay minerals) contribute to the groundwater composition. So, the chemistry of these waters is, partially, dependent on subterranean pathways.

Nicholson (1993) suggests that the majority of mineral waters, including thermal waters, have a meteoric origin. Isotopic analyses carried out in mineral waters of NW Portugal support a meteoric origin (Lima, 2001, 2010). During subterranean course, water interacts with wall rock and obtains its dissolved load. On the contrary, Marques (1999) and Calado (2002) sustain a deeper origin, from magmatic hot volatile fluxes. This origin is justified by the presence of mineralizing compounds such as CO_2 , H_2S , Br, Cl and F, in carbonic and sulphur waters.

Marques et al. (2003) studied the Caldas do Moledo geothermal site (HCO_3^- -Na type water) in the Douro River valley (NW Portugal) and showed how geochemical and isotopic data were used to constrain recharge areas, groundwater flow paths, and mixing between deep geothermal fluids and shallow cold groundwater. The most abundant lithotypes are metasedimentary rocks, granites and aplite-pegmatite veins. Water-rock interaction studies have greatly contributed to a conceptual hydrogeological circulation model from the Cabeço de Vide region, Central Portugal (Marques et al., 2008). These waters with HCO_3^- -Ca/Mg composition would be responsible for the serpentinization of fresh ultramafic rocks (dunites) present at depth.

In another hydrogeological environment (limestone aquifer of Caldas da Rainha, central Portugal), Marques et al. (2010) used chemical and isotopic data to assess potential sites for future well drilling and development. These thermomineral waters belong to the Cl-Na sulphurous-type. The presence of HCO_3^- , Ca^{2+} (and Mg^{2+}) are related to water-limestone interactions, while Na^+ , Cl^- and SO_4^{2-} concentrations are mainly associated with the dissolution of halite and gypsum. Special emphasis was put on the characterization of local/regional flow paths and the interaction between shallow cold water ($\sim 17^\circ\text{C}$) and warm thermomineral groundwater ($\sim 33^\circ\text{C}$). Sonney and Vuataz (2010) studied in detail a sulphurous spring emerging along a complex fault system. Fracture network and hydrothermal alterations have an important role in the modification of porosity and permeability of the granite (Fritz et al., 2010; Ledésert et al., 2010).

Lima (2010) discusses the origin and composition of the Caldas de Saúde thermomineral water in granite rocks. This water, of meteoric origin, has a prolonged and deep subterranean circuit. It has a Cl-Na composition but it is, also, of sulphurous type.

Published studies by Frapé et al. (1992), Blyth et al. (2000) and Iwatsuki et al. (2002), on calcite in granite fracture infillings and its isotopic composition showed the influence of fluids in the origin of these carbonates.

Several studies in the NW region of Portugal were carried out on granite weathering (Sequeira Braga et al., 2002) and also on hydrogeology (Lima, 2001). Preliminary work was carried out by Lima (2004) concerning the relationship between granite secondary minerals and the groundwater geochemical characteristics.

Although the sulphurous springs are abundant in the CIZ Portuguese, research on these springs has been directed particularly to the origin and chemical composition of these waters. These studies have not been adequately complemented with studies of the mineralogy of the surrounding rock weathering. In fact, our methodological approach is different from previous studies carried out in Portugal.

In this article, we present a study of the Terras de Bouro granite weathering, the fracture network infillings, superficial water and groundwater chemical composition and, also, the origin of the sulphur spring. The mineralogical composition of the fracture infillings and the uncommon argillitic weathering of the granite, close to the mineral water spring and their complex geological conditions explain the location of the sulphur spring.

The secondary minerals were studied to know the alteration type (weathering or hydrothermal) that could play an important role in the water-rock interactions and, particularly, clay-calcite-solution interactions on the granitic body. Besides the scientific interest of this research, the present study had a practical interest since it was part of a water exploration program. This program finished with the recent opening (in May 2010) of the “Termas de Moimenta” spa, contributing to the socio-economic development of the region.

2. Presentation of the study area

2.1. Geomorphological and geological setting

The study area is located in the Terras de Bouro region (Fig. 1a) and includes, in particular, the Devesa River drainage basin. The mineral water occurrence (sulphur spring) is located on the left bank of the Devesa River. The geomorphology of the Minho Province is strongly influenced by an intense fracture network. Sloping terrains characterize the study area with high peaks contrasting with “V” valleys with steep slopes (Fig. 1b). The bedrock of this area is coarse-grained porphyritic granite, calc-alkaline and biotite-rich, crossed by a set of basic dikes, usually strongly weathered, quartz dikes and granitic pegmatite dikes. The granite is also crossed by an intense fracture network, which defines the regional lineaments east-west, ENE-WSW, north-south and NNW-SSE (Fig. 1c).

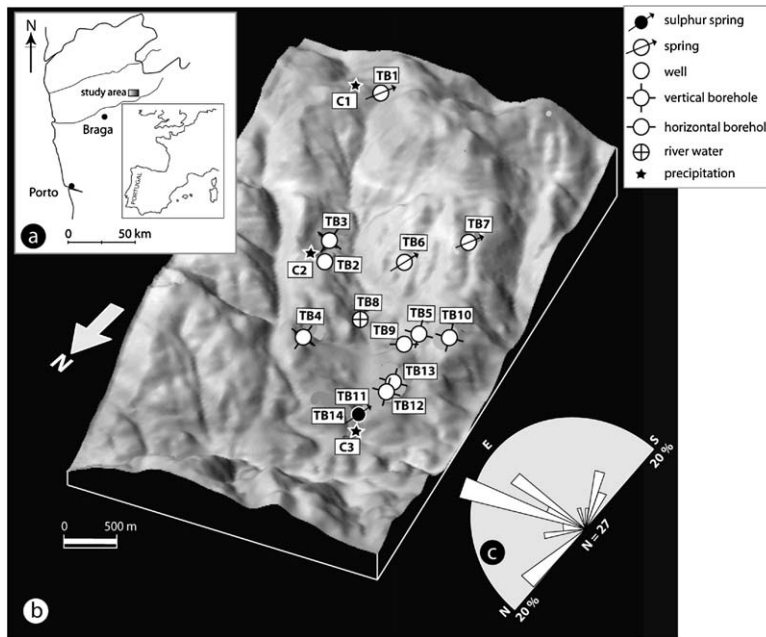


Fig. 1. (a) Location of the study area; (b) 3D illustration of geomorphology of the Terras de Bouro region, hydromineral spring location and water sampling points. Universal transverse mercator (UTM) coordinates, 29, ED50; (c) directional frequency of the major lineaments.

Fig. 1. (a) Localisation de la zone d'étude ; (b) représentation 3D de la géomorphologie de la région de Terras de Bouro, localisation de la source hydrominérale et sites d'échantillonnage des eaux. Coordonnées UTM, 29, ED50 ; (c) fréquence directionnelle des linéaments majeurs.

Field data confirm that the great regional lineaments are related to the late-D₃ (the third deformation phase of the Variscan orogeny—approximately 300 Ma ago) brittle deformation that gives some control on the granite weathering mechanisms. The different weathering levels are represented in a thematic map (Fig. 2).

Granitic saprolites are the dominant weathering facies in the area (Fig. 2). Fresh rock outcrops (only at the Devesa and Gordeiras Rivers) and the weathered rocks seem to be controlled by NNW–SSE dextral strike-slip faults, east–west faults (locally, with oblique-slip–normal and right kinematics) and ENE–WSW faults. Related to these fault systems, frequently, basic dikes and, rarely, granitic pegmatites and quartz dikes occur. The contact through faults, among different weathering levels (e.g., weathered rocks and granitic saprolites), was observed in some outcrops (Fig. 2).

In the studied area the regional pattern of the granite weathering process (Sequeira Braga et al., 2002) does not occur in the sulphur spring. An intense argillitic alteration occurs representing a singular occurrence in the regional setting. The cross-section A–A' (Fig. 3a) shows the vertical distribution of the weathering granite levels of Terras de Bouro (Lima, 2004). In this cross-section, the saprolites thickness is 15 m.

The location of the mineral water occurrence is defined by a dextral strike-slip ductile–brittle shear zone NNW–SSE (Fig. 3b and c), responsible for the development of a tilted extensional structure – gash fractures oriented near a north–south trend (Fig. 3b) that, with a late reactivation, generated a Riedel–structure with oblique-slip – normal and right kinematics (Fig. 3b, c and d). In this shear zone,

centimetre-scale veins filled with clay minerals and calcite, occur which are called in this study “clay and calcite veins”.

2.2. Hydrogeology

The sulphur spring is located on the Devesa River drainage basin oriented along one of the most important structural directions (NNW–SSE). The hydrographic network is highly controlled by brittle structures (Fig. 2). According to Lima (2001, 2010) the occurrence of localised hydrogeological systems in fractured media, such as in granitic terrains, justifies that this study could be confined to the Devesa River drainage basin.

The recharge takes place by infiltration of rainwater. In the study area, the mean annual precipitation is approximately 2500 mm (Lima, 2001). Groundwater flow essentially occurs through the fracture network and in the granite saprolite. Groundwater discharge basically occurs through springs and wells. In the Devesa River drainage basin, the sulphur spring is the only mineral water occurrence, with a discharge average value of 0.3 L/s.

3. Materials and methods

Eleven samples of weathered granite and fracture infillings were collected in the discharge zone. The sampling was carried out attending to changes of granitic alteration facies, structures and textures observed in the field. Horizontal sampling was done to cross the veins filled by clay and calcite. The studied profile is 2.5 m deep at the outcrop and the sulphur spring occurs in the lower part

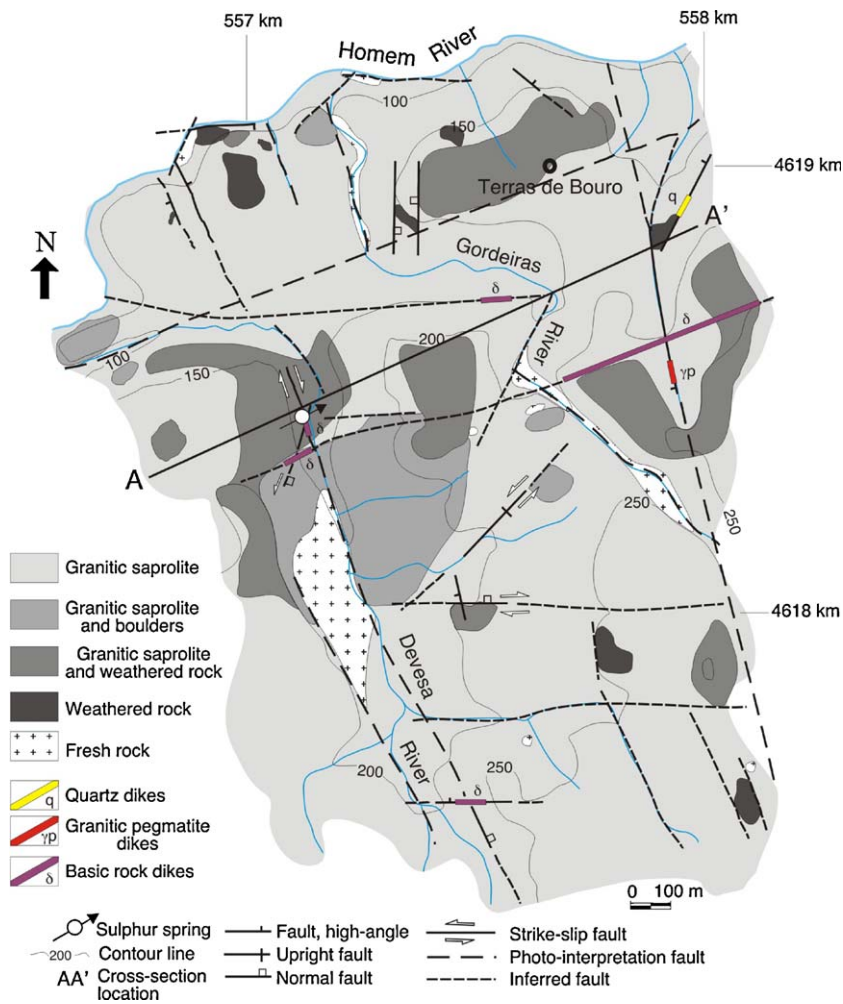


Fig. 2. Geological setting of the Terras de Bouro granite weathering levels around the sulphur spring: thematic map (1/10,000). The km values refer to UTM coordinates.

Fig. 2. Carte géologique simplifiée des niveaux d'altération météorique du granite de Terras de Bouro autour de la source sulfureuse : carte thématique (1/10 000). Les valeurs en kilomètres s'appliquent aux coordonnées UTM.

(Fig. 4). These materials were examined by optical microscopy, X-ray diffraction (XRD), scanning electron microscopy (SEM) with an energy dispersive spectrometer (EDS) for chemical analysis, using secondary X-rays and standard ZAF corrections that allow semi-quantitative microanalyses and characterization of mineralogical phases. SEM observations were carried out with a LEICA Cambridge S360 microscope. The mineralogy was determined using a Philips PW1710 (APD, 3.6 j version) diffractometer (40 kV, 20 mA) with $\text{CuK}\alpha$ radiation. The step size was $0.02^\circ 2\theta$ and the counting time was 1.25 s. The bulk mineralogy was determined by random powders and clay fraction was determined on material $< 2 \mu\text{m}$ in size. The XRD analyses were carried out on air-dried, ethylene glycol-solvated and heated (490°C) oriented samples on glass slides.

The studies by optical microscopy and SEM-EDS were carried out on polished thin sections and also on weathered rock fragments, granitic sapolite and fracture fillings.

Samples of groundwater, surface water and rainwater were collected on the Devesa River basin (Fig. 1). This sampling included springs (four samples, including sulphur waters), one well, vertical boreholes (six samples), one horizontal borehole, and two samples on the Devesa River. Six samples of rainwater were collected from three stations at 100, 300 and 600 meters elevation. Rainfall samples were collected weekly in March (2002). In the case of the groundwater and surface waters, the samples were collected between June and July (2002).

Two bottles for each water sample were used, one for alkalinity determination and the other for the remaining parameters (cations and anions). In the field, pH, Eh (mV, direct measure Ag-AgCl electrode), electrical conductivity ($\mu\text{s}/\text{cm}$) and temperature ($^\circ\text{C}$), were determined from groundwater and surface water samples, using a WTW-model P4 multiparametric equipment.

Isotopic analyses of $\delta^{18}\text{O}$ and $\delta^2\text{H}$ and dissolved inorganic C (DIC) from sulphur water (one sample) and $\delta^{18}\text{O}$ and $\delta^{13}\text{C}$ from fracture fillings (two samples) were

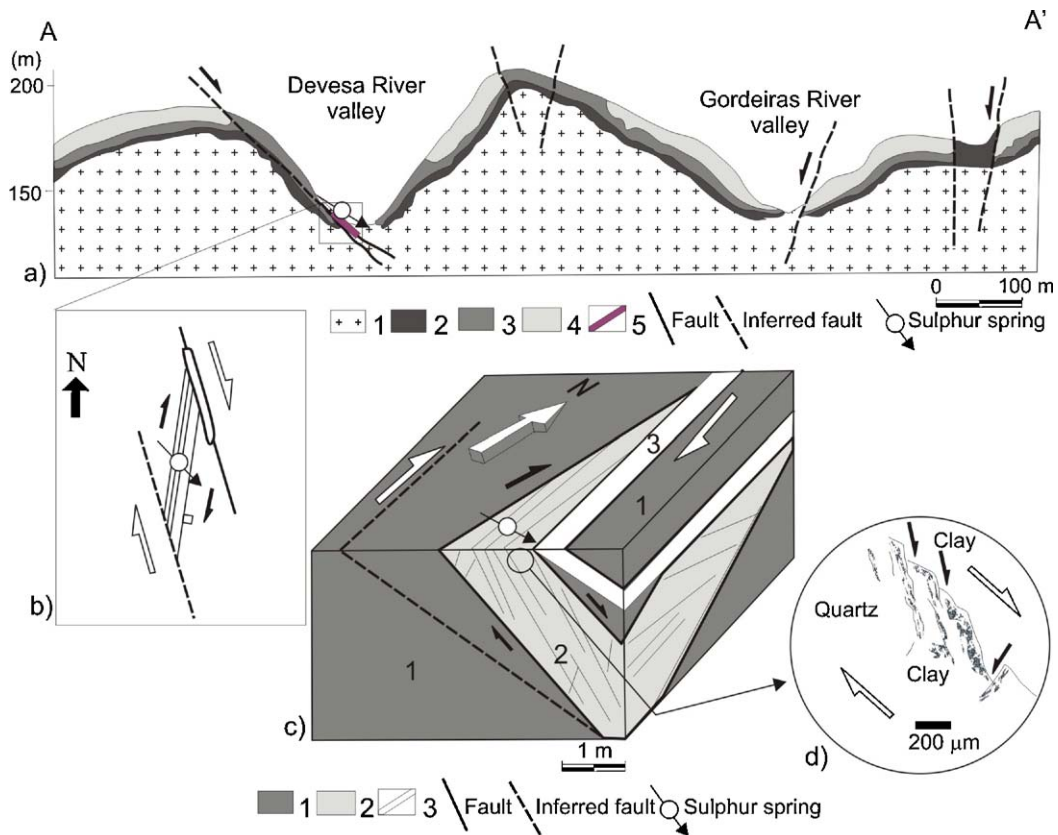


Fig. 3. Sulphur spring geological setting: (a) cross-section A-A' (see Fig. 2): 1: granite (fresh rock); 2: weathered rock; 3: granitic saprolite and weathered rock; 4: granitic saprolite; 5: basic rock dike; (b) 2D interpretative scheme of the structure; (c) 3D schematic interpretative structure: 1: granitic saprolite and weathered rock; 2: fault gouge and clay and calcite veins; 3: basic rock dike; (d) Riedel structure (scheme by optical microscope).

Fig. 3. Cadre géologique de la source sulfureuse : (a) coupe géologique A-A' (voir Fig. 2) : 1 : granite (roche saine) ; 2 : roche altérée ; 3 : saprolite (arène) et roche altérée ; 4 : saprolite ; 5 : dyke de roche basique ; (b) structure interprétative schématique 2D : 1 : saprolite et roche altérée, 2 : argile de faille et veines d'argile et calcite, 3 : structure Riedel (schéma au microscope polarisant).

carried out at the Actlabs-Activation Laboratories Ltd (Ontario, Canada). All samples were collected in the sulphur water discharge zone. The sulphur water sample was collected by using two bottles, one for DIC analysis and another one for deuterium and $\delta^{18}\text{O}$ analysis. Fracture filling carbonate minerals were selected under a binocular microscope. The mineralogical composition and purity of the samples were verified by XRD. All samples were analysed using thermal ionization mass spectrometry (TIMS). The results are reported in Table 1, using the conventional δ – notation with respect to the VPDB standard for $^{13}\text{C}/^{12}\text{C}$ and VSMOW standard for $^{18}\text{O}/^{16}\text{O}$ (Clark and Fritz, 1997). The precision of isotopic analyses is $\pm 0.2\%$ for $\delta^{18}\text{O}$ and $\delta^{13}\text{C}$ and $\pm 2\%$ for $\delta^2\text{H}$.

4. Results and discussion

4.1. Weathering of the granitic bedrock

The wall rock of the sulphur spring is a biotite-rich coarse-grained porphyritic granite composed of quartz (25–33%), K-feldspar (orthoclase or microcline, 29–32%), microcline (frequently perthitic), plagioclase (oligoclase/

andesine, 22–30%), biotite (9–14%). Muscovite (< 4%), ilmenite, ilmenorutile, apatite, zircon, monazite, titanite, thorite and fibrolite are accessory minerals (Ferreira et al., 2000; Lima, 2004). The last author shows that the hydrothermal alteration of this granite is characterized by muscovitization, albitization, silicification of feldspar crystals, biotite chloritization and an incipient kaolinization of the plagioclase crystals.

Micromorphological studies by optical microscopy and SEM-EDS analyses show the following features of the alteration of primary minerals: (i) etch-pits in quartz grains; (ii) great density of the microcline fracture network that is characterized by thin and rectilinear fractures with angular intersections or enlarged fractures filled by a smectitic or kaolinitic crystalliplasma. The incongruent dissolution of feldspar seems to be partially controlled by intrinsic factors of the mineral itself, namely, perthitic microtexture (Wilson and McHardy, 1980); (iii) kaolinite and gibbsite are associated with the high porosity of plagioclase and, rarely, smectites; (iv) distortion of cleavage surfaces of biotite by pyrite growth (Fig. 5a). Pyrite presents automorphic habits (cube and octahedron), massive or granular. Some pyrite crystals are cracked and show etch-pits on the crystal surfaces (Figs. 5b and 5d).

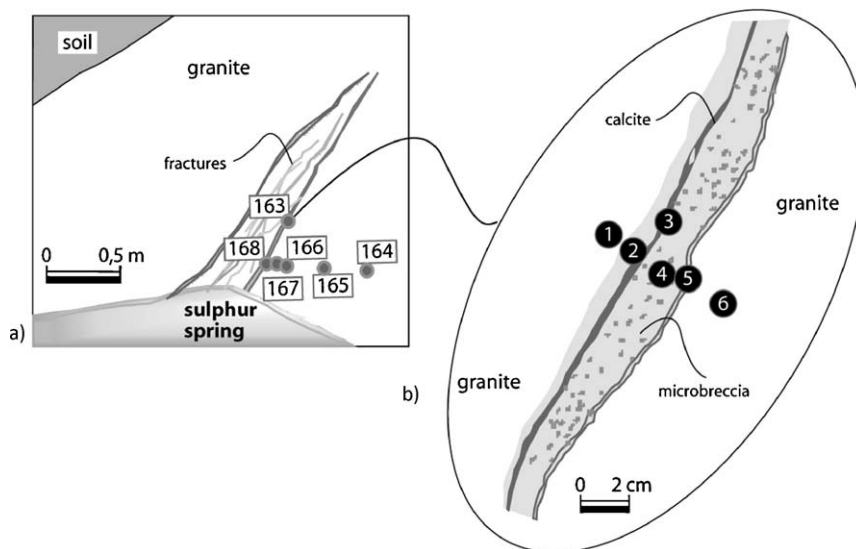


Fig. 4. (a) Sampling location on the sulphur spring zone; (b) 1: granite with pervasive argillic alteration; 2–5: clay and calcite veins; 4: microbreccia; 6: weathered granite.

Fig. 4. (a) Localisation d'échantillonnage dans la zone de la source sulfureuse ; (b) 1 : granite avec altération argileuse pervasive ; 2–5 : veines d'argile et calcite ; 4 : microbrèche ; 6 : granite altéré.

Similar textural features were reported by Iwatsuki and Yoshida (1999). These authors suggest that dissolution textures may have formed during interaction of the rock with oxidized groundwater in fractured zones. Semi-quantitative chemical analyses by SEM-EDS have shown that biotite alteration is displayed by the loss of K and Ti and by the decrease of Mg and Fe in the pyrite crystallization microsites (Fig. 5c). Ti-oxide grains are also visible along cleavage surfaces of biotite. Between exfoliated layers of biotite, kaolin minerals also appear as shown by Fig. 5b. The similar percentages of Si and Al correspond to the formation of those kaolin minerals.

Mineralogical results by XRD show that clay minerals, calcite and pyrite are the characteristic secondary minerals of the sulphur spring zone. Mineralogical composition of the weathered granite samples and clay and calcite veins that occur in the shear zone (Fig. 4) are characterised by great lateral heterogeneity. Illite; mixed-layer chlorite/smectite, illite/smectite and kaolinite/smectite; smectite; kaolinite; gibbsite; lepidocrocite and goethite, are other examples of secondary minerals that occur at adjacent profiles (~5 m) to the sulphur

spring. The clay fraction of the weathering profiles, in this environment, is about 27% of the whole rock and the skeleton is formed mostly by quartz and K-feldspar. The nature and amounts of these clay minerals, in the profiles near the sulphur spring, characterize a pervasive argillic alteration in this particular area. Considering the sulphur spring zone, the estimations of mineral quantities by XRD of the bulk rock (samples 164 to 167; Fig. 4) indicates an increase of the following secondary minerals: (i) clay minerals from 8 to 40%; (ii) calcite from 2 to 17%; and (iii) pyrite from 3 to 7%.

According to Lima (2004), the XRD patterns of the < 2 μm fraction show the 15.5 \AA basal reflection which expands to 17 \AA after ethylene-glycol treatment. The heating at 490 $^{\circ}\text{C}$ causes collapse near 10 \AA . The 060 reflection at 1.50 \AA revealed the presence of dioctahedral smectites. The XRD patterns associated with SEM-EDS analyses are consistent with the presence of montmorillonite. Lower interlayer charge and Ca and Na as main ions in the smectitic interlayer have previously been observed in the sulphur spring zone. Montmorillonite is the dominant clay mineral in the vein infilling.

Table 1

Isotopic composition of the sulphur water and calcites from fracture fillings. All the samples were collected in the sulphur emergence, –n.d.: no data. The analyses were done in the ACTLABS laboratory (Canada). The $\delta^{18}\text{O}$ (‰) is expressed with respect to the standards VPDB and VSMOW.

Tableau 1

Composition isotopique de l'eau sulfureuse et des calcites de remplissage des fractures. Tous les échantillons ont été prélevés dans la zone d'émergence sulfureuse, – n.d. : aucune donnée. Les données isotopiques proviennent du dans le laboratoire ACTLABS (Canada). Les valeurs de $\delta^{18}\text{O}$ (‰) sont exprimées par rapport aux étalons VPDB et VSMOW.

Sample	Composition	$\delta^{13}\text{C}$		$\delta^{18}\text{O}$		$\delta^2\text{H}$	
		VPDB	VPDB	VPDB	VSMOW	VSMOW	VSMOW
163 C	Calcite	–14.0	–6.1	24.62		n.d.	
168 C	Calcite	–13.6	–6.2	24.52		n.d.	
TB14	Sulphur water	n.d.	–35.76	–5.96		–32.97	
	Carbonate species of the sulphur water	–16.2	–35.87	–6.03		n.d.	

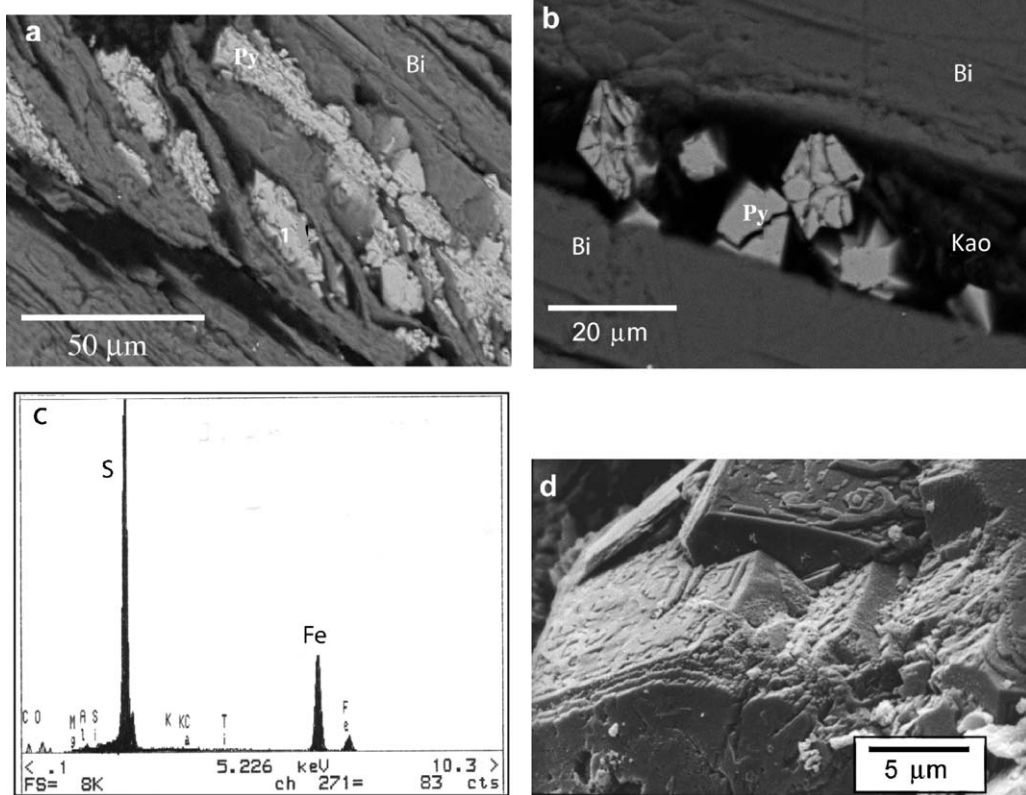


Fig. 5. SEM-EDS images of polished thin section of weathered granite (sample 166; Fig. 4): (a) pyrite (Py) between cleavage surfaces of biotite (Bi); (b) fractured pyrite crystals and kaolinite (Kao) crystallites; (c) X-rays spectrum of pyrite - position 1; (d) etch-pits on the pyrite crystal surfaces.

Fig. 5. Images SEM-EDS sur section polie de granite altéré (échantillon 166; Fig. 4) : (a) pyrite (Py) entre plans de clivage de biotite (Bi) ; (b) cristaux de pyrite fracturée et cristallites de kaolinite (Kao) ; (c) spectre de rayons-X de la pyrite – point d'analyse 1 ; (d) figures de dissolution sur la surface de cristaux de pyrite.

4.2. Fracture infillings

Sulphur water flows inside the connected fracture network (faults, joints, mineral cleavage and intra, inter- and transmineral fissures) that occurs on the NNW–SSE shear zone (Fig. 3). Clay minerals and calcite are the main secondary mineral deposits sealing these fractures. Calcite is compact or is usually in crystals in the open spaces (fractures). Crystals are varied in habit, either hexagonal mica-like (Folk, 1974), or with an elemental rhombohedral form. The morphology of these carbonates may be related to the undersaturation degree of the water in relationship to calcite and/or to the kinetic of the crystalline growth (Iwatsuki et al., 2002). According to these authors, such features reflect the water chemistry conditions, such as pH, Na and Mg concentrations, rate of carbonate supply and also crystallization rate. Montmorillonite occurs also as a mineral deposition sealing the above mentioned fractures (clay and calcite veins; Fig. 4) and those of the surrounding altered wall-rock (granite; Fig. 4).

Optical and electron microscopy (SEM-EDS) allow interpretation of the textural relationship between the precipitation of the secondary mineral deposits (calcite and montmorillonite) and the open spaces (Fig. 6a, b). Occasionally, inside the calcite porosity (Fig. 6c), mont-

morillonite is coated by a thin film of a Si-rich material. This material is not identified by XRD, due to its small amount, but its presence was confirmed by SEM-EDS. Kühnel and Van der Gaast (2000) and Christidis (2001) report that silica resulting from feldspar weathering, when not completely removed from the clay mineral crystallization environment, can cover the surface of smectite crystallites as a thin opal film.

4.3. Hydrogeochemistry

For the Devesa River basin the geochemical compositions of groundwater, surface water and rainwater are shown in Table 2. Sulphur water (TB14 sample) is the most mineralised solution of the system. The sulphur water salinity (TDS = 171.4 mg/L) is much higher than the mean value (TDS = 55.8 mg/L) of other studied groundwaters (Table 2). According to Lima (2001), the TDS values of groundwater from NW of Portugal rarely exceed 50 mg/L. This sulphur water presents an alkaline pH (9.25) and a low redox potential (–61 mV). Taking into account that sulphur water is characterised by a negative redox, the sulphur occurs predominantly as reduced species (H_2S and HS^-), being the hydrosulphuric gas identified *in situ* for its characteristic smell. However, its levels of NO_3^- and Mg^{2+}

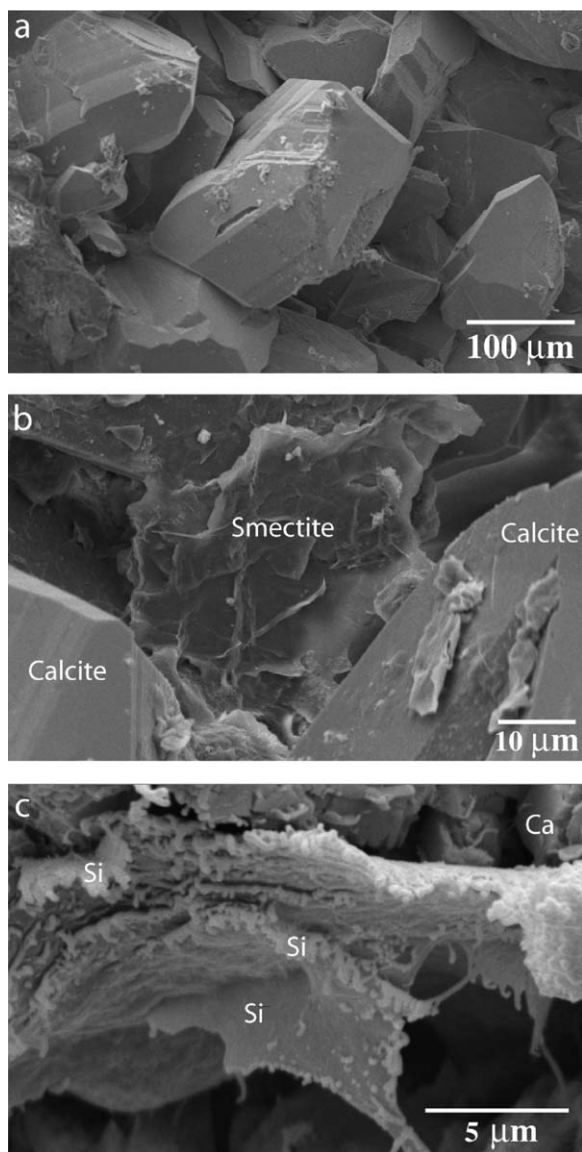


Fig. 6. SEM images of clay and calcite vein infilling (sample 163; Fig. 4): (a) calcite crystals in open spaces; (b) smectite and calcite deposits sealing fractures; (c) amorphous silica deposition on the montmorillonite edges.

Fig. 6. Images SEM du remplissage des veines d'argile et calcite (échantillon 163 ; Fig. 4) : (a) cristaux de calcite dans les espaces ouverts ; (b) remplissage des fractures par des dépôts de smectite et calcite ; (c) dépôt de silice amorphe sur les bords de la montmorillonite.

are lower than the other regional waters (Table 2). Some groundwater, collected in springs (TB1, TB6 and TB7 samples—Table 2) also present a low salinity. The geochemical composition of these groundwaters suggests a flow at shallow depth. The composition of these shallow groundwaters, and that of rainfall, can represent the chemical composition of the infiltration water in this hydrosystem (Devesa River basin). However, this infiltration water acquires mineralization along its drive and, consequently, the sulphurous water composition point to a longer circuit, being, therefore, a more evolved fluid.

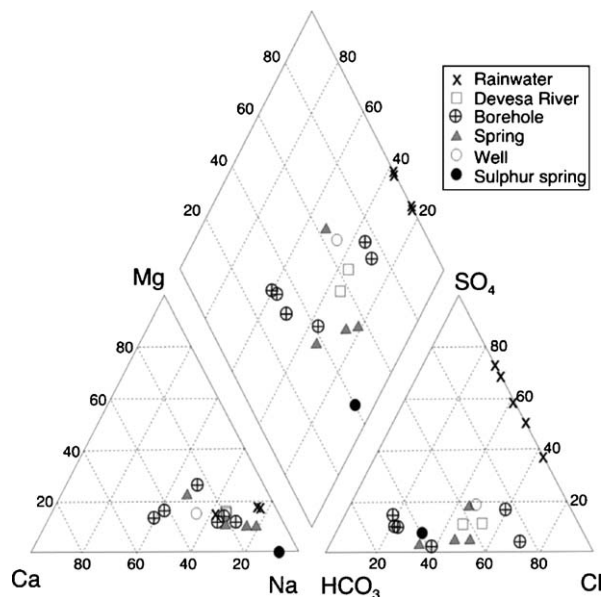


Fig. 7. Chemical analyses of water samples plotted in the Piper (1944) diagram.

Fig. 7. Analyses chimiques d'échantillons d'eaux, projetées dans le diagramme de Piper (1944).

The results of the chemical analyses in the Piper (1944) triangular diagram (Fig. 7) show that surface or shallow groundwater and deep groundwater are distributed either in the chloride or bicarbonate domains. Considering the rainwater composition of the studied area, some samples are chloride-rich or sulphate-rich. The composition of this rainwater should be related to the wind direction and to the origin of the atmospheric wet air of the rainy events. Thus, the chloride-rich water samples point to a predominantly marine origin and the sulphate-rich waters mainly to a continental origin.

The sulphur water is richer in Na than regional waters, which are of the calcium-magnesium type (Fig. 7). Among the latter, the more superficial rainwater and shallow groundwater (spring water) are plotted near the Na pole and the deeper groundwater (boreholes) is plotted near the Ca and Mg poles. These data are consistent with the geochemical evolution of the granite bedrock, during weathering of the rock-forming minerals, particularly, plagioclase and biotite.

The fresh rock is already altered by metasomatic events, namely feldspar perthitization and albitization and incipient argillitization of the plagioclase, as was mentioned above. Beyond this alkaline metasomatism, the fissures pattern defines geochemical microsystems that allow the solutions to flow and, consequently, the advance of an early hydrothermal alteration. The chemistry of groundwater can also be controlled at depth by the plagioclase dissolution. A possible ion exchange reaction with Na-bearing minerals like montmorillonite crystallizing in the plagioclase etch pits could also take place, as verified by Hounslow (1995) and Iwatsuki and Yoshida (1999), according to whom the enrichment of Na and depletion

Table 2

Chemical composition of groundwater, surface waters and rainwater of the Devesa River basin (Fig. 1b). TDS-total dissolved solids; b.d., below detection; n.d., no data. The composition of the sulphur water spring is in bold.

Tableau 2

Composition chimique de l'eau souterraine, de l'eau superficielle et de l'eau de pluie du bassin du fleuve Devesa (Fig. 1b). TDS-solides totaux dissous ; b.d. : au-dessous de la limite de détection ; n.d. : aucune donnée. La composition de l'eau de la source sulfureuse est en gras.

Sample	EC ($\mu\text{S}/\text{cm}$)	pH	Eh (mV)	T ($^{\circ}\text{C}$)	TDS (mg/L)	CO ₂ (mg/L)	Ca ²⁺ (mg/L)	Mg ²⁺ (mg/L)	Na ⁺ (mg/L)	K ⁺ (mg/L)	Al ³⁺ (mg/L)	HCO ₃ ⁻ (mg/L)	SO ₄ ²⁻ (mg/L)	Cl ⁻ (mg/L)	NO ₃ ⁻ (mg/L)	F ⁻ (mg/L)	Br ⁻ (mg/L)	SiO ₂ (mg/L)	Σ cations (meq/L)	Σ anions (meq/L)
TB1	29.9	6.29	256	13.9	30.2	9.0	1.23	0.42	4.38	b.d.	0.02	10.70	0.39	3.40	0.40	0.07	b.d.	13.50	0.29	0.29
TB2	43.9	5.72	325	13.4	33.3	17.8	1.99	0.62	4.08	1.27	0.043	5.70	2.50	4.50	6.30	b.d.	b.d.	8.58	0.37	0.37
TB3	61.6	5.89	320	13.9	46.8	11.4	1.72	0.72	6.29	3.03	0.065	5.42	3.15	7.70	8.90	0.04	b.d.	12.00	0.50	0.52
TB4	85.1	6.19	309	14.5	61.9	9.5	2.27	1.01	10.80	2.14	0.042	8.93	1.29	14.79	8.77	0.03	b.d.	15.40	0.73	0.73
TB5	108.0	6.69	279	15.0	83.8	10.8	4.66	3.08	10.70	1.20	0.014	32.28	3.98	5.98	10.22	0.69	b.d.	23.90	0.98	0.98
TB6	29.5	6.03	288	12.7	28.5	12.1	0.77	0.32	4.43	0.40	0.018	7.90	0.60	4.40	0.70	b.d.	b.d.	12.10	0.27	0.28
TB7	25.2	6.29	339	12.7	21.8	5.0	0.50	0.27	4.09	b.d.	b.d.	5.90	0.58	4.10	0.50	b.d.	b.d.	8.26	0.23	0.23
TB8	36.9	6.38	284	15.3	30.7	5.7	1.19	0.61	4.74	0.60	b.d.	8.40	1.70	5.30	1.30	b.d.	b.d.	10.20	0.33	0.34
TB9	64.2	5.85	341	16.5	50.8	21.0	3.13	1.36	5.61	1.63	0.01	9.07	3.49	6.45	10.53	b.d.	b.d.	13.20	0.55	0.57
TB10	56.3	6.20	315	14.3	51.7	19.7	2.39	0.74	7.20	1.26	b.d.	19.00	0.50	7.50	0.00	b.d.	b.d.	20.70	0.53	0.53
TB11	40.5	6.42	297	15.8	32.1	4.4	1.29	0.68	4.99	0.60	b.d.	7.10	1.80	6.10	2.40	b.d.	b.d.	10.00	0.35	0.36
TB12	134.9	6.54	289	17.1	100.3	23.2	11.94	2.20	11.20	0.50	0.041	49.10	6.00	8.40	4.70	1.27	b.d.	24.60	1.28	1.31
TB13	134.3	6.54	261	16.6	105.2	22.3	10.48	2.49	12.10	0.70	b.d.	47.20	8.62	7.14	2.60	2.40	b.d.	30.40	1.27	1.32
TB14	255.0	9.25	-61	16.8	171.4	0.1	3.50	0.03	52.30	0.62	0.012	62.80	9.5	19.90	0.00	9.00	0.23	37.90	2.47	2.27
TBC1.1	29.8	4.36	n.d.	n.d.	n.d.	n.d.	0.28	0.11	0.92	b.d.	n.d.	b.d.	4.47	1.51	2.27	0.02	b.d.	b.d.	0.06	0.17
TBC1.2	28.0	4.75	n.d.	n.d.	n.d.	n.d.	0.17	0.29	2.52	b.d.	n.d.	b.d.	5.63	4.01	0.94	b.d.	b.d.	b.d.	0.14	0.25
TBC2.1	23.9	4.56	n.d.	n.d.	n.d.	n.d.	0.25	0.11	0.80	b.d.	n.d.	b.d.	4.98	1.37	1.71	0.01	b.d.	b.d.	0.06	0.17
TBC2.2	23.9	4.68	n.d.	n.d.	n.d.	n.d.	0.13	0.25	2.15	b.d.	n.d.	b.d.	6.55	3.31	0.78	0.01	b.d.	b.d.	0.12	0.24
TBC3.1	15.1	4.80	n.d.	n.d.	n.d.	n.d.	0.12	b.d.	0.66	b.d.	n.d.	b.d.	4.31	1.10	1.08	0.01	b.d.	b.d.	0.03	0.14
TBC3.2	22.8	4.66	n.d.	n.d.	n.d.	n.d.	0.13	0.23	1.99	b.d.	n.d.	b.d.	2.66	3.31	0.75	b.d.	b.d.	b.d.	0.11	0.16

Table 3

Log of saturation indices (SI) of the waters calculated for different minerals, using the PHREEQE program (Parkhurst et al., 1980). n.d., no data, due to the absence or contents lower than the detection limit; K-F–microcline; Ca-Mont–Ca-Montmorillonite. The SI values of the sulphur water spring is in bold.

Tableau 3

Log des indices de saturation (IS) des eaux, calculés pour différents minéraux, en appliquant le programme PHREEQE (Parkhurst et al., 1980). n.d., aucune donnée, dû à l'absence à des teneurs inférieures à la limite de détection ; K-F - microcline ; Ca-Mont - Ca-Montmorillonite. Les valeurs de IS de l'eau de la source sulfureuse sont en gras.

Sample	K-F ^a	Albite ^b	Quartz ^c	Illite ^d	Ca-Mont ^e	Chlorite ^f	Kaolinite ^g	Gibbsite ^h	Amorphous ⁱ	Amorphous ^j	Calcite ^k
TB1	n.d.	-2.99	0.5	n.d.	3.53	-23.66	5.32	1.77	-1.02	-0.84	-4.04
TB2	-2.3	-4.28	0.31	-0.12	2.42	-29.49	4.73	1.67	-1.13	-1.03	-4.69
TB3	-1.11	-3.27	0.45	1.32	3.51	-26.47	5.46	1.89	-0.9	-0.89	-4.61
TB4	-0.38	-2.15	0.55	2.58	4.64	-21.73	6.20	2.16	-0.63	0.79	-3.97
TB5	-0.62	-2.14	0.73	1.35	3.11	-15.76	4.48	1.12	-1.66	-0.60	-2.61
TB6	-1.93	-3.39	0.47	0.60	3.25	-27.35	5.24	1.76	-1.04	-0.88	-4.65
TB7	n.d.	n.d.	0.31	n.d.	n.d.	n.d.	n.d.	n.d.	n.d.	-1.04	-4.70
TB8	n.d.	n.d.	0.36	n.d.	n.d.	n.d.	n.d.	n.d.	n.d.	-0.98	-4.05
TB9	-1.99	-3.9	0.45	-0.16	2.17	-25.9	4.23	1.27	-1.5	-0.87	-4.13
TB10	n.d.	n.d.	0.68	n.d.	n.d.	n.d.	n.d.	n.d.	n.d.	-0.66	-3.60
TB11	n.d.	n.d.	0.34	n.d.	n.d.	n.d.	n.d.	n.d.	n.d.	-0.99	-4.04
TB12	-1.56	-2.64	0.71	0.04	2.22	-18.20	3.69	0.74	-2.03	-0.61	-2.15
TB13	n.d.	n.d.	0.87	n.d.	n.d.	n.d.	n.d.	n.d.	n.d.	-0.51	-2.23
TB14	0.17	-0.35	0.82	-0.25	0.15	-3.2	1.11	-0.66	-3.43	-0.50	-0.04

^a KAlSi_3O_8 .

^b $\text{NaAlSi}_3\text{O}_8$.

^c SiO_2 .

^d $\text{K}_{0.6}\text{Mg}_{0.25}\text{Al}_{12.3}\text{Si}_{3.5}\text{O}_{10}(\text{OH})_2$.

^e $\text{Ca}_{0.1165}\text{Al}_{12.33}\text{Si}_{3.67}\text{O}_{10}(\text{OH})_2$.

^f Chlorite (14 Å) $\text{Mg}_5\text{Al}_{12}\text{Si}_3\text{O}_{10}(\text{OH})_8$.

^g $\text{Al}_2\text{Si}_2\text{O}_5(\text{OH})_2$.

^h $\text{Al}(\text{OH})_3$.

ⁱ Amorphous aluminium $\text{Al}(\text{OH})_3$.

^j Amorphous silica SiO_2 .

^k CaCO_3 .

of Mg in groundwater of fractured granitic rocks similar to those we studied is due to ion exchange.

Table 3 provides the results of the saturation indices of the groundwater, using the geochemical model PHREEQE (Parkhurst et al., 1980), in order to understand the water–rock interactions.

Most of the studied waters (Table 3), including sulphur water (TB14 sample), are undersaturated with respect to plagioclase and to microcline, according to the calculated saturation index (SI). In water samples, the supersaturation can be verified with respect to quartz. Concerning the secondary minerals, the supersaturation related to Ca-montmorillonite and kaolinite and the undersaturation with respect to chlorite and gibbsite were verified. The SI also indicates that all groundwater samples have a tendency to dissolve calcite while the sulphur water is in equilibrium with this mineral. These results are consistent with the mineralogical composition of clay and calcite in the veins.

All samples are undersaturated with respect to amorphous silica. In the spring zone, as mentioned above, it was observed that the montmorillonite is coated with thin films of a Si-rich material, which occurs in very small amounts (Fig. 6c). Based on their textural features these films are probably composed of amorphous silica, which would precipitate at the thermodynamic conditions of the sulphur spring.

To understand the origin of the water mineralization, mainly of the sulphur water, where water–rock interaction has an important role, either by dissolution of the granite

primary minerals, or by ion exchange reactions between clay minerals and water, two diagrams of chemical element variations are discussed below.

Taking account that the chloride ion is a good hydrological cycle tracer (Cl^- is a conservative ion), the variations and correlations between Cl and Na for all water samples analysed (Table 2) are shown in Fig. 8. These results revealed that rainwater samples define an alignment with a slope (1.7148) close to the slope (1.7986) of

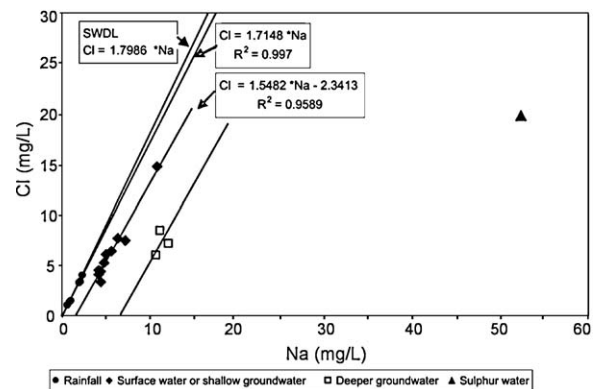


Fig. 8. Cl vs Na diagram of all water sampling points from the Devesa River basin. Sea water dilution line (SWDL).

Fig. 8. Diagramme Cl vs Na de tous les points d'échantillonnage des eaux du bassin du fleuve Devesa. Ligne de dilution de l'eau de mer (SWDL).

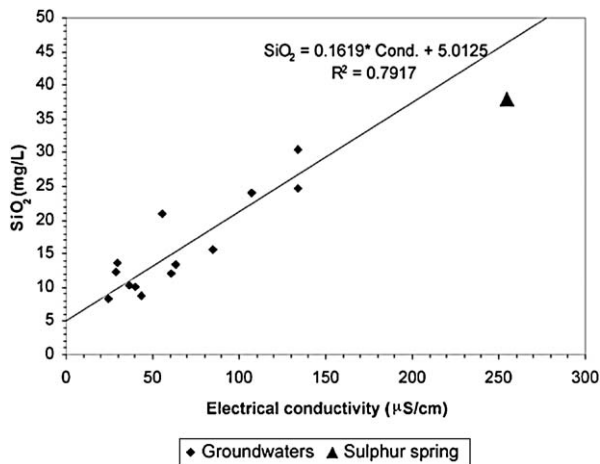


Fig. 9. SiO_2 vs Electrical conductivity diagram of groundwater and sulphur spring samples.

Fig. 9. Diagramme SiO_2 vs Conductivité électrique de l'échantillonnage des eaux souterraines et de la source sulfureuse.

the sea water dilution line (SWDL), meaning that only a 2.4% difference exists.

Regarding to shallow groundwater (collected in springs and shallow boreholes) and surface waters (collected on the river and in the absence of recent rainwater) the variations of the ion concentrations define an alignment subparallel to the rainwater mentioned above. This alignment is translated in the direction of an increase of the Na concentration. Similarly, groundwater flowing at a greater depth, also shows the same behaviour. This increase of Na concentration supports the role of the water–rock interaction in water samples. This water–rock interaction explains the global water mineralization of the sulphur water.

In Fig. 9, values of SiO_2 concentration and electrical conductivity were plotted. The hydrolysis of aluminosilicate minerals, mainly plagioclases, delivers to the water, other elements as ionic species (e.g., Ca^{2+} , Mg^{2+} , Na^+), besides silica (Fig. 6c). This means that the increase of the amounts of Ca^{2+} , Mg^{2+} , Na^+ , in particular, controls the electrical conductivity of the aqueous solution. Silica is present, essentially, as non-ionic species and, for that reason it does not contribute to the electrical conductivity of the water in the pH conditions of all analysed samples (except sulphur water where the pH is 9.25).

Taking into account the sulphur water pH (9.25) some amount of silica is present as trihydrogenosilicate (H_3SiO_4^-) and, consequently, also contributes to the increase of the electrical conductivity of the water.

4.4. Isotope geochemistry

To determine the origin (meteoric or deeper) of the sulphur water and the possible genetic relationship between this fluid and calcites that occur as fracture fillings on the discharge zone, an isotopic study was made. In Table 1, the results of isotopic compositions of both samples are given: $\delta^{18}\text{O}$ and $\delta^2\text{H}$ of sulphur water and $\delta^{18}\text{O}$ and $\delta^{13}\text{C}$ of carbonate species of the water and also of the calcite.

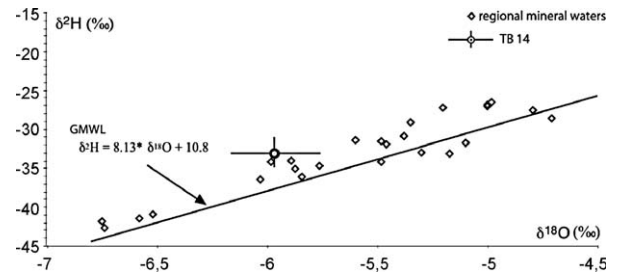


Fig. 10. $\delta^2\text{H}$ vs $\delta^{18}\text{O}$ diagram of sulphur water (TB 14). Other mineral waters from the Minho Province (Lima, 2001) are shown for comparison. Global Meteoric Water Line (GMWL).

Fig. 10. Diagramme $\delta^2\text{H}$ vs $\delta^{18}\text{O}$ de l'eau sulfureuse (TB14). D'autres eaux de la Province de Minho (Lima, 2001) sont projetées par comparaison. Droite de l'eau météorique globale (GMWL).

The isotopic composition ($\delta^2\text{H}$ and $\delta^{18}\text{O}$) of the sulphur water, plotted on Fig. 10, is close to the global meteoric water line (GMWL), which means a predominantly meteoric origin of this water. This result is corroborated by those previously presented by Lima (2001) about the mineral water isotopic composition from the Minho Province (Fig. 10).

According to Lima (2004), the application of Na/K and silicon geothermometers suggests a reservoir temperature estimated between 90 and 110 °C. Furthermore, the presence of F (9 mg/L) and Br (0.23 mg/L) compared with its absence in the other waters of the Devesa River basin (Table 2), indicates a greater interaction between the water and the granite body, associated with a long residence time and deeper circulation. This fact is supported by the negative redox potential (–61 mV) of this thermomineral environment.

The plotting of $\delta^{18}\text{O}$ close to the GMWL suggests that this water does not show significant variations in its isotopic composition during the subterranean pathway. However, the slight depletion in $\delta^{18}\text{O}$ of the sulphur water (Fig. 10) may be due to the incorporation of the ^{18}O in calcite and clay minerals, predominantly montmorillonite, that fill the fractures (clay and calcite veins) in which sulphur fluid flows. According to Hoefs (1997), minerals with predominance of Si–O–Si and C–O–C bonds, namely quartz, K-feldspar, calcite and Na/Ca-rich plagioclase, tend to include, preferentially, the heavy oxygen. Temperature, residence time and water–rock interaction are other factors that control a possible ionic exchange.

The isotopic composition of the calcite is related to: (i) the water isotopic composition from which it was precipitated; (ii) the dissolved inorganic carbon (DIC) species (HCO_3^- predominantly); (iii) the temperature, whereas the isotopic fractionation of the ^{18}O is especially dependent on temperature (Iwatsuki et al., 2002). In this way, the isotopic composition of $\delta^{18}\text{O}$ calcites provides a powerful parameter to determine the fluid temperature. Taking into account that the isotopic composition $\delta^{13}\text{C}$ of calcite is a good tracer (Hoefs, 1997; Iwatsuki et al., 2002) this isotopic composition suggests the inorganic carbon source of the sulphur water.

The theoretical values of DIC from which calcite precipitated were calculated using the isotopic fraction-

ation factor between DIC species of the water and the calcite, according to the following equation (Emrich et al., 1970):

$$\alpha_{\text{calcite-water}} = (^{13}\text{C}/^{12}\text{C})_{\text{calcite}} / (^{13}\text{C}/^{12}\text{C})_{\text{water}} \quad (1)$$

In terms of δ values, this equation becomes:

$$\alpha_{\text{calcite-water}} = 1000 + \delta^{13}\text{C}_{\text{calcite}} / 1000 + \delta^{13}\text{C}_{\text{water}} \quad (2)$$

According to Eq. (2) and using the isotopic fractionation factor (α) between calcite and water ($\alpha = 1.00185$ at 20 °C, Emrich et al., 1970), the theoretical $\delta^{13}\text{C}$ values calculated for DIC are -15.82% (sample 163 C) and -15.42% (sample 168 C). Both $\delta^{13}\text{C}$ calculated values for calcite samples are very close to the analytical value (-16.2%) obtained from DIC from sulphur water (Table 1). These data suggest that calcites are precipitated from carbonate species in the sulphur water. Considering the $\delta^{13}\text{C}$ values of some important carbon reservoirs, according to Hoefs (1997), the calcite $\delta^{13}\text{C}$ isotopic signature (-14% , Table 1) is compatible with a carbon source from DIC species in non-marine organisms or in freshwater, like the studied sulphur water, where total dissolved solid contents are low (TDS $<< 1000$ mg/L)–Table 2.

The source of DIC present in the sulphur water could result, essentially, from the dissolution of $\text{CO}_{2(g)}$ from soil during the infiltration of water in the unsaturated zone, because the concentration of CO_2 in the soil, resulting from biological activity, is approximately 10 to 100 times higher than in the atmosphere (Clark and Fritz, 1997). The dissolution of CO_2 into the water causes a series of reactions from hydration to dissolution, leading to the formation of several species of DIC ($\text{CO}_{2(aq)}$, H_2CO_3 , HCO_3^- and CO_3^{2-}). The reactions contribute, at the same time, with H^+ for the hydrolysis of the silicates. The distribution of DIC species is set by the pH (Clark and Fritz, 1997; Konhauser, 2006). Therefore, for pH value ~ 9 of the studied sulphur water, determined in the spring, the major DIC species are HCO_3^- and CO_3^{2-} . The enrichment of the $\delta^{13}\text{C}$ of calcite (-14%), when compared with the $\text{CO}_{2(g)}$ theoretical value of the soil (-23%), can be explained by the different isotope fractionation factors, being distinct for several carbonate species present in the water. The majority of the plants in the study area follow the C3 photosynthesis and, according to Cantolla (2003), these plants have lower values of $\delta^{13}\text{C}$, between -22% and -30% .

From the $\delta^{18}\text{O}$ values of the calcite and of the sulphur water (Table 1 and Fig. 10), it is possible to determine the temperature of calcite formation using the $\delta^{18}\text{O}$ as geothermometer (Blyth et al., 2000). Plotting these values on Fig. 11, a temperature near 17 °C was estimated. Also, a similar value (17.02 °C) was calculated using the following equation (O'Neil et al., 1969):

$$1000 \ln \alpha_{\text{calcite-water}} = 2.78 (10^6 T^{-2}) - 3.39 \quad (3)$$

α being the factor of isotope fractionation between calcite and water and T the temperature in Kelvin.

These temperatures [Fig. 11 and Eq. (3)] are similar to the mean value measured in the discharge zone (Table 2).

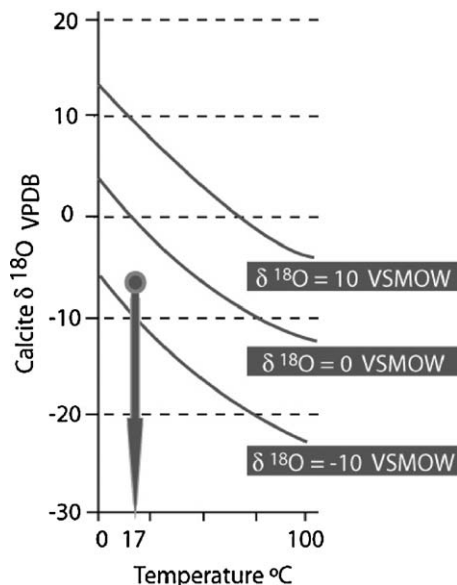


Fig. 11. Plotting of calcite $\delta^{18}\text{O}$ values and of the water from which calcite precipitated. The horizontal axis corresponds to the aqueous solution temperature. Curve plotting (+10 and -10 VSMOW) represents the water $\delta^{18}\text{O}$ composition (modified after Frapet et al., 1992).

Fig. 11. Projection des valeurs $\delta^{18}\text{O}$ de la calcite et de l'eau, à partir de laquelle la calcite a été précipitée. L'axe horizontal correspond à la température de la solution aqueuse. La courbe tracée (+10 et -10 VSMOW) représente la composition $\delta^{18}\text{O}$ de l'eau (modifié d'après Frapet et al., 1992).

On the basis of the available data, calcite from clay and calcite veins was originated from sulphur water at temperature conditions close to those at the surface. In this way, it is likely that they have a meteoric origin. For the montmorillonite (whose studies are still in progress) the first result is $\delta^{18}\text{O}_{\text{VSMOW}} = 21\%$. Using this value and the value of sulphurous water as geothermometer, we obtained a temperature of ~ 25 °C. This result suggests, also, a meteoric origin for the smectite.

4.5. Mineralogical and geochemical model of the sulphur spring zone

In Fig. 12 is shown a sketch of a sulphur spring that occurs in the Terras de Bouro granite, related to a brittle shear zone, with its mineralogical and geochemical behaviour.

Pyrite occurs in wall rock of clay and calcite veins. Pyrite can be formed from the reaction of the Fe leached from biotite with reduced S, in the form of H_2S and HS^- , transported by sulphur waters. Calcite is also the main secondary mineral deposit sealing the fractures in the shear zone. The morphology of this carbonate reflects the water chemistry conditions, such as pH, Na and Mg concentrations, rate of carbonate supplying and also the crystallization rate. Montmorillonite, with a lower interlayer charge and Ca and Na as main ions in the smectite interlayer, is the dominant clay mineral in the vein infilling.

Montmorillonites analysed by SEM-EDS (Lima, 2004) show compositional variations, which may reflect the

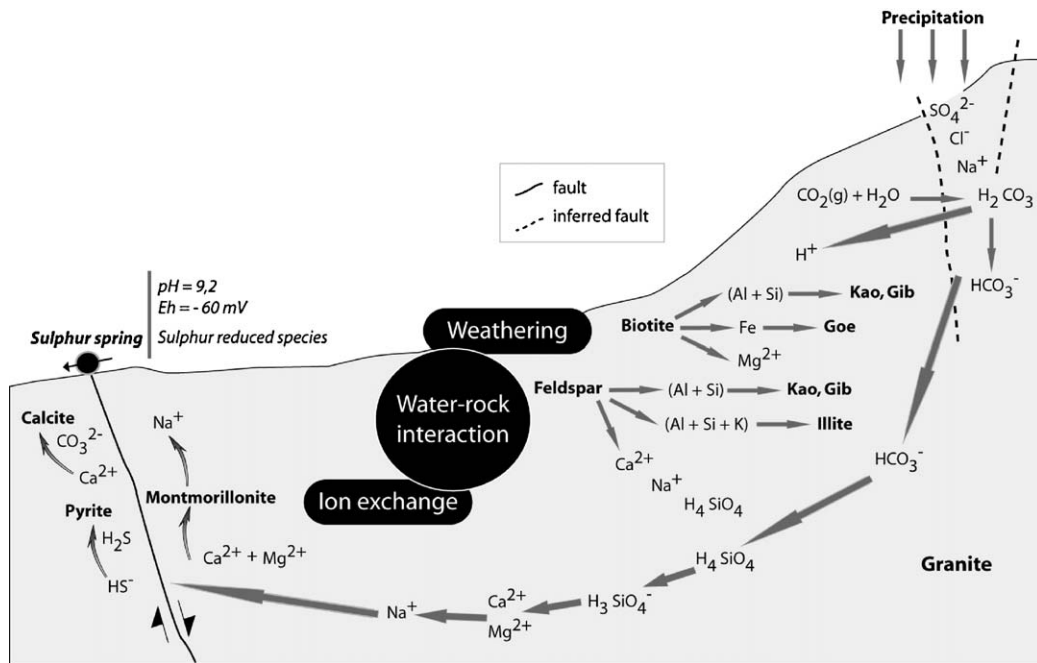


Fig. 12. Geochemical and mineralogical model of the sulphur spring zone, representative of the water–rock interaction. Kaolinite (kao); gibbsite (Gib); goethite (Goe).

Fig. 12. Modèle géochimique et minéralogique de la zone de la source sulfureuse, représentant l'interaction eau–roche. Kaolinite (kao), gibbsite (Gib), goethite (Goe).

influence of microenvironment conditions, but all of them present a dioctahedral character and are, dominantly, low-charge montmorillonites. The interlayer Ca and Na contents range from 0.06 to 0.32 a.p.f.u. and 0.0 to 0.73 a.p.f.u., respectively. It is not precluded that this clay mineral may occur in the same fracture system at greater depth, considering that the dioctahedral smectites are stable up to 100 °C. The studied smectite was collected at the surface, at the site where the sulphur spring emerges, because we had not access to a deeper sampling. This clay mineral is associated with: (i) fractures of the shear zone that lead to sulphurous water per ascensum; (ii) confined to a microfissural system of low hydraulic conductivity, which was observed in intra-mineral fissures (microcline and plagioclase) of the granite.

The geochemistry of the sulphur water, namely its high pH, presence of sulphur reduced species and low redox potential, justifies the occurrence of those mineralization in the spring zone. It cannot be excluded that such mineralization occurs at depth, filling the same fracture network.

5. Conclusions

The Terras de Bouro sulphur spring is located on the Devesa River basin (NW Portugal) in a late-Variscan ductile-brittle shear zone. In this shear zone, clay and calcite veins occur, crosscutting the granite bedrock. The unique occurrence of smectite associated with an argillitic alteration (< 2 µm fraction is 29% in average) was observed in a shear zone where the sulphur spring emerges.

Pyrite, calcite and clay minerals are the characteristic secondary minerals of the mineral water occurrence (sulphur spring).

This sulphur water is considered the most evolved groundwater of the hydrosystem of the Devesa River basin. Its high salinity, the enrichment in Na (52.30 mg/L) and the almost absence of Mg (0.03 mg/L) compared to regional groundwater, suggest a greater degree of rock–water interaction that could include an ionic exchange between clay minerals, mainly montmorillonite, and water.

The deeper regional waters are of the Ca–Mg type. The shallow waters (rainwater and spring) have higher levels of Na than Ca, but a much lower level than that of the sulphur water. Therefore, the enrichment in Na can be explained by the weathering reactions on primary minerals such as plagioclases, but Na–(Ca, Mg) ion exchange between secondary minerals like montmorillonite and groundwater could not be completely excluded even still not really demonstrated here. This would suppose an uptake of Ca and Mg from water by clay minerals, while the latter could supply previously adsorbed Na of the smectitic interlayer to the solution.

The greater degree of rock–water interaction could be related to a deeper circuit and a flow during a more prolonged period of time with respect to the other local groundwaters.

The recharge of this hydrogeological system is mostly from rainwater. The isotopic signatures $\delta^2\text{H}$ and $\delta^{18}\text{O}$ of sulphur water indicate that its origin is predominantly meteoric, being the result of mixing a deeper fluid with shallower groundwater.

The isotopic signature $\delta^{13}\text{C}$ (-14‰) of the calcite indicates that the ^{13}C has its origin from the carbonates of the sulphur water. The application of the $\delta^{18}\text{O}$ geothermometer on the basis of the isotopic signature $\delta^{18}\text{O}$ of calcite and of carbonate species of sulphur water suggest that calcite has been precipitated in the thermodynamic conditions of the emergence, $\sim 17^\circ\text{C}$. The isotopic signature $\delta^{18}\text{O}$ of smectite suggests, also, a meteoric origin of the water.

The textural relationships between calcite and montmorillonite precipitated in the clay and calcite veins show that these minerals have the same origin.

Acknowledgements

Partial funding to the authors was provided by the Centro de Investigação Geológica, Ordenamento e Valorização de Recursos that is supported by the Pluriannual program of the Fundação para a Ciência e a Tecnologia, funded by the European Union (FEDER program) and the national budget of the Portuguese Republic. Very insightful and helpful comments were made by Bertrand Fritz and by Gh. de Marsily, for which we are grateful. We also thank H el ene Paquet for her suggestions to improve this paper.

References

- Blyth, A., Frapce, S., Blomqvist, R., Nissinen, P., 2000. Assessing the past thermal and chemical history of fluids in crystalline rock by combining fluid inclusion and isotopic investigations of fracture calcite. *Appl. Geochem.* 15, 1417–1437.
- Calado, C., 1993.  guas sulf reas alcalinas e gasocarb nicas na Pen nsula Ib rica: Distribui o e controlo geotect nico. Com. XII Reuni o Oeste Peninsular 1, 235–245.
- Calado, C., 2002. A ocorr ncia de  guas sulf reas alcalinas no Maci o Hesp rico: quadro hidrogeol gico e quimiog nese. PhD Thesis, Universidade de Lisboa, Lisboa. 462 p.
- Cantolla, A.U., 2003. Historia del Clima de la Tierra. Servicio Central de Publicaciones del Gobierno Vasco, 306 p.
- Clark, I., Fritz, P., 1997. Environmental Isotopes in Hydrogeology. Lewis Publishers, New York, 328 p.
- Christidis, G.E., 2001. Formation and growth of smectites in bentonites: a case study from Kimolos Island, Aegean, Greece. *Clays and Clay Minerals* 49, 204–215.
- Emrich, K., Enhalt, D.H., Vogel, J., 1970. Carbon isotope fractionation during the precipitation of calcium carbonate. *Earth Planet. Sci. Lett.* 8, 363–371.
- Ferreira, N., Dias, G., Meireles, C., Sequeira Braga, M.A., 2000. Carta Geol gica de Portugal na escala de 1/50 000. Not cia explicativa da folha 5-D (Braga) Instituto Geol gico e Mineiro, Lisboa, 68 p.
- Folk, R.L., 1974. The natural history of crystalline calcium carbonate: effect of magnesium content and salinity. *J. Sed. Petrol.* 44, 40–53.
- Frapce, S.K., Blomqvist, R., Nissinen, P., Blyth, A., McNutt, R.H., 1992. The geochemistry of fracture filling calcite at the Olkiluoto research site, Southwest Finland. In: Blomqvist, R., Nissinen, P., Frapce, S.K. (Eds.), Dating of Fracture Minerals from Olkiluoto SW Finland. Industrial Power Company. TVO Site Investigations. Working Report, 166 p.
- Fritz, B., Jacquot, E., Jacquemont, B., Baldeyrou-Bailly, A., Rosener, M., Vidal, O., 2010. Geochemical modelling of fluid-rock interactions in the context of the Soultz-sous-For ts geothermal system. *C. R. Geoscience* 342, 653–667.
- Hoefs, J., 1997. Stable Isotope Geochemistry. Springer-Verlag, Berlin, 201 p.
- Hounslow, A.W., 1995. Water Quality Data. Analysis and Interpretation. Lewis Publishers, New York, 397 p.
- Iwatsuki, T., Yoshida, H., 1999. Groundwater chemistry and fracture mineralogy in the basement granitic rock in the Tono Uranium Mine Area, Gifu, Japan - Groundwater composition, Eh evolution analysis by fracture filling minerals. *Geochem. J.* 33, 19–32.
- Iwatsuki, T., Satake, H., Metcalfe, R., Yoshida, H., Hama, K., 2002. Isotopic and morphological features of fracture calcite from granitic rocks of Tono Area, Japan: a promising palaeohydrogeological tool. *Appl. Geochem.* 17, 1241–1257.
- Konhauser, K., 2006. Introduction to geomicrobiology. Blackwell Publishing, United Kingdom, 425 p.
- K hnel, R.A., Van der Gaast, S.J., 2000. Inhomogeneous clay mineral formation in volcanic rocks from Gran Canaria Spain: preliminary results. In: Gomes, C.S.F. (Ed.), Proceeding of the First Latin-American Clay Conference, 1. Funchal, pp. 15–26.
- Led sert, B., Hebert, R., Genter, A., Bartier, D., Clauer, N., Grall, C., 2010. Fractures, hydrothermal alterations and permeability in the Soultz Enhanced Geothermal System. *C. R. Geoscience* 342, 607–615.
- Lima, A.S., 2001. Hidrogeologia de Terrenos Gran ticos. PhD Thesis, Universidade do Minho, Braga, 451 p.
- Lima, A., 2010. Composi o e origem das  guas minerais naturais—exemplo de Caldas da S ude. Almedina (Ed.), Coimbra, 246 p.
- Lima, M.F., 2004. As altera es do granito de Terras de Bouro associadas a uma nascente sulf rea. MSc Thesis, Universidade do Minho, Braga, 158 p.
- Marques, J., 1999. Geoqu mica dos fluidos e da interac o  gua-rocha: os casos das  guas mineralizadas quentes e frias de Chaves, Vilarelho da Raia, Vidago e Pedras Salgadas. PhD Thesis, Instituto Superior T cnico, Universidade T cnica de Lisboa, Lisboa, 276 p.
- Marques, J.M., Espinha Marques, J., Carreira, P.M., Gra a, R.C., Aires-Barros, L., Carvalho, J.M., Chamin , H.L., Borges, F.S., 2003. Geothermal fluids circulation at Caldas do Moledo area, northern Portugal: geochemical and isotopic signatures. *Geofluids* 3, 189–201.
- Marques, J.M., Carreira, P.M., Carvalho, M.R., Matias, M.J., Goff, F.E., Basto, M.J., Gra a, R.C., Aires-Barros, L., Rocha, L., 2008. Central Portugal. Origins of high pH mineral waters from ultramafic rocks. *Appl. Geochem.* 23, 3278–3289.
- Marques, J.M., Eggenkamp, H.G.M., Gra a, H., Carreira, P.M., Matias, M.J., Mayer, B., Nunes, D., 2010. Assessment of recharge and flowpaths in a limestone thermomineral aquifer system using environmental isotope tracers (central Portugal). *Isotopes Environ. Health Stud.* 46 (2), 156–165 Taylor & Francis (Edt).
- Nicholson, K., 1993. Geothermal fluids - chemistry and exploration techniques. Springer-Verlag, Berlin, 263 p.
- O’Neil, J.R., Clyton, R.N., Mayeda, T.K., 1969. Oxygen isotope fractionation in divalent metal carbonates. *J. Chem. Physics* 51, 5547–5558.
- Parkhurst, D.L., Thorstenson, D.C., Plummer, L.N., 1980. PHREEQE - A computer program for geochemical calculations. U.S. Geological Survey Water Resource Invest. 80–96.
- Piper, A.M., 1944. Graphical procedure in the geochemical interpretation of water-analyses. *Am. Geophys. Union Trans.* 25, 914–923.
- Sequeira Braga, M.A., Paquet, H., Begonha, A., 2002. Weathering of granites in temperate climate (NW Portugal): granitic saprolites and arenization. *Catena* 49, 41–56.
- Sonney, R., Vuataz, F.D., 2010. Remobilisation of deep Na-Cl waters by a regional flow system in the Alps: Case study of Saint-Gervais-les-Bains (France). *C. R. Geoscience* 342, 151–161.
- Wilson, M.J., McHardy, W.J., 1980. Experimental etching of microcline perthite and implications regarding natural weathering. *J. Microsc.* 120 (3), 291–302.